

Optimization, Standardization, and Testing of a New NMR Method for the Determination of Zeolite Host–Organic Guest Crystal Structures

Colin A. Fyfe* and Darren H. Brouwer†

Contribution from the Department of Chemistry, University of British Columbia, R300,
6174 University Boulevard, Vancouver, British Columbia, Canada V6T 1Z3

Received January 31, 2006; E-mail: fyfe@chem.ubc.ca

Abstract: An optimized and automated protocol for determining the location of guest sorbate molecules in highly siliceous zeolites from ^{29}Si INADEQUATE and $^1\text{H}/^{29}\text{Si}$ cross polarization (CP) magic-angle spinning (MAS) NMR experiments is described. With the peaks in the ^{29}Si MAS NMR spectrum assigned to the unique Si sites in the zeolite framework by a 2D ^{29}Si INADEQUATE experiment, the location of the sorbate molecule is found by systematically searching for sorbate locations for which the measured rates of $^1\text{H}/^{29}\text{Si}$ cross polarization of the different Si sites correlate linearly with $^1\text{H}/^{29}\text{Si}$ second moments calculated from H–Si distances. Due to the $^1\text{H}/^{29}\text{Si}$ cross polarization being in the “slow CP regime” for many zeolite–sorbate complexes, it is proposed that the CP rate constants are best measured by $^1\text{H}/^{29}\text{Si}$ cross polarization drain experiments, if possible, to avoid complications that may arise from fast ^1H and ^{29}Si $T_{1\rho}$ relaxations. An algorithm for determining the sorbate molecule location is described in detail. A number of ways to effectively summarize and display the large number of solutions which typically result from a prediction of the structure from the CP MAS NMR data are presented, including estimates of the errors involved in the structure determinations. As a working example throughout this paper, the structure of the low loaded *p*-dichlorobenzene/ZSM-5 complex is determined under different conditions from solid-state $^1\text{H}/^{29}\text{Si}$ CP MAS NMR data, and the solutions are shown to be in excellent agreement with the known single-crystal X-ray diffraction structure. This structure determination approach is shown to be quite insensitive to the use of relative rate constants rather than absolute values, to the detailed structure of the zeolite framework, and relatively insensitive to temperature and motions.

Introduction

The size and shape selectivities which zeolite molecular sieves exhibit toward organic molecules are central to their numerous commercial and industrial applications. In particular, they exhibit selectivity in determining the size and shape of the products formed in catalytic reactions, the rates at which molecules are adsorbed into and diffuse through their frameworks, and the preferred locations of guest molecules within the host framework. To fully understand the interactions between the guest molecule and the zeolite framework which give rise to this size and shape selectivity, with the ultimate goal of theoretically modeling these systems in a reliable manner, it is necessary to have reliable structures of a number of these zeolite–sorbate host–guest complexes.

Diffraction experiments are conventionally the method of choice to determine the structures of crystalline materials. However, at present, there are very few reliable structures of zeolite–sorbate complexes as the use of single crystal X-ray diffraction (XRD) is limited to the very few zeolite types for which single crystals of suitable size and quality can be grown.

For most zeolites, the crystal dimensions are on the order of a few micrometers, and therefore diffraction techniques are generally limited to powder samples for which reliably locating the weakly scattering organic guest molecules is much more difficult due to the more limited data sets obtained. The notable exception is the zeolite ZSM-5 or Silicalite-1 (MFI framework topology¹), for which single crystals of sufficient size and quality for single crystal XRD can be easily synthesized. Consequently, this zeolite has been the focus of most structural investigations of zeolite–guest molecule complexes. A very limited number of reliable crystal structures of sorbate–zeolite complexes of ZSM-5 are available from the single-crystal XRD studies by van Koningsveld and co-workers.^{2–7}

Because diffraction experiments are generally limited in their application to locating guest molecules in zeolite hosts, we have developed strategies based on solid-state nuclear magnetic

† Present address: National Research Council of Canada, Steacie Institute for Molecular Sciences, 100 Sussex Drive, Ottawa, Ontario, Canada K1A 0R6. Darren.Brouwer@nrc-cnrc.gc.ca.

- (1) Baerlocher, C.; Olson, D. H.; Meier, W. M. *Atlas of Zeolite Framework Types*, 5th ed.; Elsevier: Amsterdam, 2001.
- (2) van Koningsveld, H.; Tuinstra, F.; van Bekkum, H.; Jansen, J. C. *Acta Crystallogr.* **1989**, *B45*, 423.
- (3) van Koningsveld, H.; Jansen, J. C. *Microporous Mater.* **1996**, *6*, 159.
- (4) van Koningsveld, H.; Jansen, J. C.; de Man, A. J. M. *Acta Crystallogr.* **1996**, *B52*, 131.
- (5) van Koningsveld, H.; Jansen, J. C.; van Bekkum, H. *Acta Crystallogr.* **1996**, *B52*, 140.
- (6) van Koningsveld, H.; Koegler, J. H. *Microporous Mater.* **1997**, *9*, 71.
- (7) van Koningsveld, H. *J. Mol. Catal. A: Chem.* **1998**, *134*, 89.

resonance (NMR) methods to determine the structures of these complexes. Solid-state NMR can provide structural information that is complementary to diffraction experiments and is independent of crystal size. The general strategy consists of three steps: (1) assignment of the ^{29}Si resonances to specific Si sites of the zeolite framework by performing two-dimensional (2D) correlation experiments, (2) experimentally determining the strengths of the distance-dependent dipolar interactions between the nuclei of the guest species and the nuclei of the zeolite framework, and (3) using this distance information to locate the guest species with respect to the zeolite framework to give the complete three-dimensional structure.

For isolated pairs of nuclei, precise distance measurements can be made. Thus in previous publications,^{8–11} the general strategy outlined above was used to locate the fluoride ions in as-made zeolites synthesized from fluoride-containing media. The peaks in the ^{29}Si spectrum were first assigned from a two-dimensional INADEQUATE experiment, after which $^1\text{H}/^{19}\text{F}/^{29}\text{Si}$ triple resonance cross polarization (CP), REDOR, and TEDOR experiments were performed to measure F–Si internuclear distances to various Si sites of the zeolite framework, from which the exact locations of the fluoride ions with respect to the zeolite framework were determined.¹⁰

Since the nuclear spin systems in zeolite–sorbate complexes are usually much more complex than isolated spin pairs, it is therefore not possible by CP or REDOR to measure precise individual internuclear distances. However, under the conditions we have employed, this general solid-state NMR strategy for structure determinations can still be extended to these systems by correlations to second moments. Its application to the high- and low-loaded complexes of the *p*-xylene/ZSM-5 system has recently been described and its viability demonstrated.^{12,13} (Eckert and co-workers have shown in related work that multispin effects in REDOR experiments on glasses can be similarly described.^{14–16}) In the case of the zeolite complexes, with the peaks in the ^{29}Si spectrum assigned from a two-dimensional INADEQUATE experiment, $^1\text{H}/^{29}\text{Si}$ CP MAS NMR experiments were performed to probe the strengths of the ^1H – ^{29}Si dipolar couplings between ^1H nuclei of (partially deuterated) *p*-xylene molecules and the ^{29}Si nuclei in the zeolite framework. For the high-loaded complex, for which the crystal structure was known, it was demonstrated that the experimentally measured rates of cross polarization were proportional to the calculated heteronuclear dipolar coupling second moments. This proportionality between the measured rates of cross polarization and calculated second moments formed the basis of an approach previously used to determine the location of the *p*-xylene guest molecules in the low-loaded form of the *p*-xylene/ZSM-5 complex from the $^1\text{H}/^{29}\text{Si}$ CP MAS NMR data.

The location determined by solid-state NMR was found to be in excellent agreement with the structure found in a subsequent independent single-crystal XRD study.¹⁷

The aim of the present work is to expand and improve upon this previous study,¹³ particularly with regard to steps 2 and 3 in the general strategy described above. Cross polarization dynamics and the measurement of CP rate constants are discussed. It is proposed that these rate constants are best measured by the cross polarization “drain” experiment to avoid complications due to fast ^1H $T_{1\rho}$ relaxation and to account for ^{29}Si $T_{1\rho}$ relaxation.¹⁸ An optimized and automated algorithm for determining the guest molecule location based on the relationship between the measured CP rate constants and the calculated heteronuclear second moments is described in detail. A number of ways to effectively summarize and display the large numbers of closely related solutions which typically result from the determination of the structure from the CP MAS NMR data are presented, including estimates of the errors involved in the structure determination. This NMR structure determination approach is shown to be relatively insensitive to the use of relative CP rate constants rather than absolute values, to the exact framework structure, and to temperature and motions, at least for the system studied. As a working example throughout this paper, the structure of the low-loaded complex of *p*-dichlorobenzene (pDCB) in ZSM-5 is determined from solid-state $^1\text{H}/^{29}\text{Si}$ CP MAS NMR data obtained under a variety of conditions and compared to the previously determined single-crystal XRD structure.⁴

The longer-term goal of this work is to first establish the reliability of this solid-state NMR method by checking the correctness of predicted structures with single-crystal XRD determinations before applying these techniques to zeolite–sorbate systems where the use of single-crystal XRD is precluded. From a database of such structures, parameterizations of the functions describing the nonbonding interactions between organic sorbates and zeolite frameworks could be reliably tested and refined so that, in the future, zeolite–sorbate host–guest structures can be successfully modeled in cases where neither NMR nor diffraction techniques are applicable.

Experimental Section

Sample. A very highly siliceous and crystalline sample of ZSM-5 was used which had peak widths of about 0.1 ppm in the ^{29}Si MAS NMR spectrum.¹⁹ The zeolite–sorbate complex was prepared by accurately weighing out the appropriate amount of organic solid and mixing with about 200 mg of calcined zeolite powder in a prescored glass ampule, giving a loading of approximately 3.5 molecules of pDCB per unit cell of ZSM-5. The ampule was evacuated on a vacuum line, flame-sealed, and then placed in an oven at about 80–100 °C for at least 12 h to equilibrate.

Solid-State NMR. Solid-state NMR experiments were carried out on a Bruker AVANCE DSX-400 NMR spectrometer operating at frequencies of 400.13 MHz for ^1H and 79.495 MHz for ^{29}Si , using a Bruker double-frequency CP MAS probe modified with a standard 7-mm stator system from Doty Scientific. ^{29}Si chemical shifts were referenced to tetramethylsilane using Q_8M_8 ²⁰ as a secondary reference by setting the highest field peak to -109.7 ppm. Low-temperature MAS was achieved by using precooled nitrogen gas as the bearing gas and

(8) Fyfe, C. A.; Lewis, A. R.; Chézeau, J. M.; Grondey, H. *J. Am. Chem. Soc.* **1997**, *119*, 12210.

(9) Fyfe, C. A.; Lewis, A. R.; Chézeau, J. M. *Can. J. Chem.* **1999**, *77*, 1984.

(10) Fyfe, C. A.; Brouwer, D. H.; Lewis, A. R.; Chézeau, J. M. *J. Am. Chem. Soc.* **2001**, *123*, 6882.

(11) Darton, R. J.; Brouwer, D. H.; Fyfe, C. A.; Villaescusa, L. A.; Morris, R. E. *Chem. Mater.* **2004**, *16*, 600.

(12) Fyfe, C. A.; Diaz, A. C.; Lewis, A. R.; Chézeau, J.-M.; Grondey, H.; Kokotailo, G. T. In *Solid State NMR Spectroscopy of Inorganic Materials*; Fitzgerald, J. J., Ed.; ACS Symposium Series 717, American Chemical Society: Washington, DC, 1999; pp 283–304.

(13) Fyfe, C. A.; Diaz, A.; Grondey, H.; Lewis, A. R.; Förster, H. *J. Am. Chem. Soc.* **2005**, *127*, 7543.

(14) Bertmer, M.; Eckert, H. *Solid State Nucl. Magn. Reson.* **1999**, *15*, 139.

(15) Chan, J. C. C.; Eckert, H. *J. Magn. Reson.* **2000**, *140*, 170.

(16) Strojek, W.; Kalwei, M.; Eckert, H. *J. Phys. Chem. B* **2004**, *108*, 7601.

(17) Lewis, A. Ph.D. Thesis, University of British Columbia, 1998.

(18) Fyfe, C. A.; Brouwer, D. H.; Tekely, P. *J. Phys. Chem. A* **2005**, *109*, 6187.

(19) Fyfe, C. A.; O'Brien, J. H.; Strobl, H. *Nature* **1987**, *326*, 281.

(20) Agaskar, P. A. *Inorg. Chem.* **1990**, *29*, 1603.

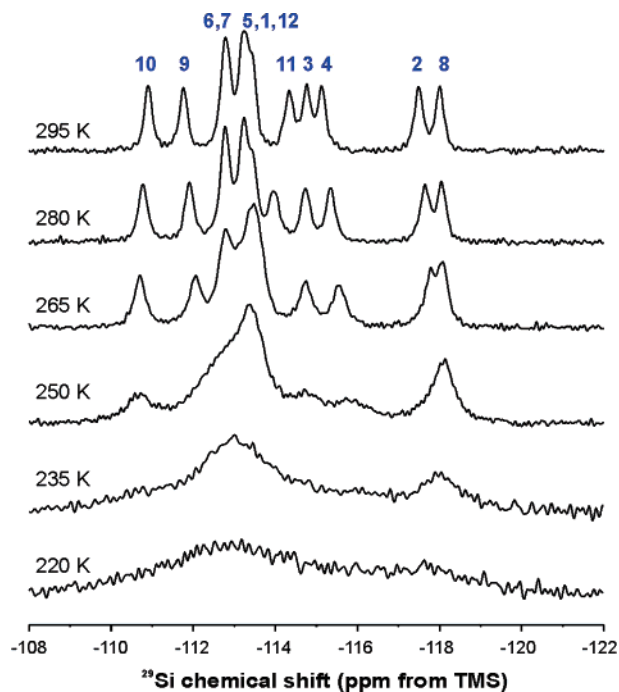


Figure 1. Quantitative variable temperature ^{29}Si MAS NMR spectra of the low-loaded pDCB/ZSM-5 complex. The spectra were acquired with 32 scans, 45° pulses, 30 s recycle delays with a spinning rate of 2 kHz. The numbers above the peaks indicate the peak assignments obtained from the 2D INADEQUATE spectrum (see Figure 2).

room-temperature air as the drive gas with the temperature controlled and monitored by a heater–thermocouple system in the probe. The Hartmann–Hahn CP match condition for $^1\text{H}/^{29}\text{Si}$ CP was initially set up on the Q_8M_8 reference sample and subsequently checked on the sample itself. The power levels corresponding to the maximum of a relatively broad matching profile were approximately 30 kHz for both ^1H and ^{29}Si . ^1H decoupling applied during the acquisition time was found to have no noticeable effect on the width of the peaks in the ^{29}Si spectrum, even at the lowest temperatures used, so it was not applied (with the exception of the mixing and evolution times in the ^{29}Si INADEQUATE experiment). All spectra were collected using a spinning rate of approximately 2 kHz. Additional experimental details for the individual spectra are provided in the figure captions.

Data Analysis. The deconvolution of the spectra, fitting of the CP and CP drain curves, and implementation of the structure determination algorithm were performed using programs written for *Mathematica*, version 3.0.²¹

Results and Discussion

1. Solid-State NMR Results. The protocol developed to determine the location of organic sorbate molecules in zeolites from $^1\text{H}/^{29}\text{Si}$ CP MAS NMR data will be described in detail using data obtained for the low-loaded pDCB/ZSM-5 complex. To establish the reliability of this protocol, the results of this NMR structure determination will be compared to a previously reported single-crystal XRD structure of this complex.⁴

Variable-Temperature NMR. A series of ^{29}Si MAS NMR spectra at different temperatures were first collected to identify the temperature at which the ^{29}Si spectrum has the most peaks resolved (Figure 1). These spectra indicate that there are 12 unique Si sites in the zeolite as expected for the orthorhombic $Pnma$ space group. However, as the temperature is lowered,

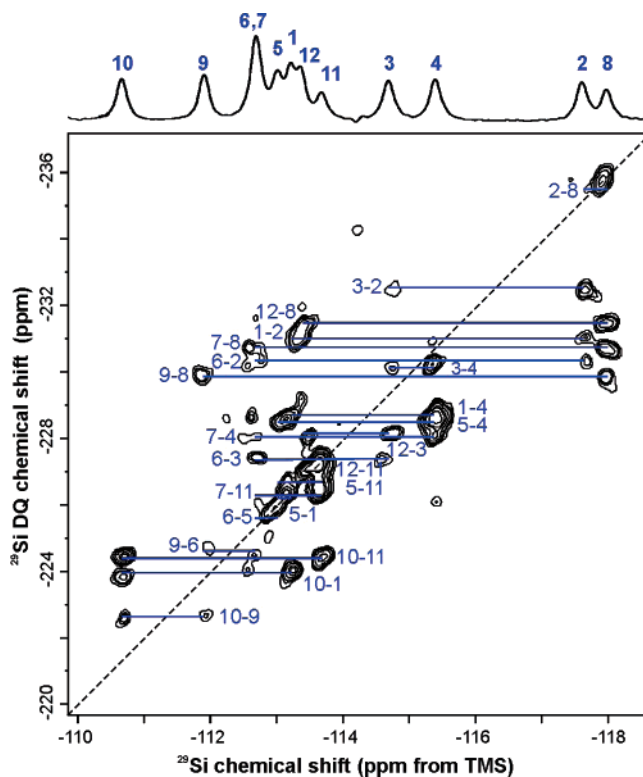


Figure 2. Two-dimensional ^{29}Si MAS INADEQUATE spectrum of the low-loaded pDCB/ZSM-5 complex at 275 K (on a sample with a slightly different loading): 48 increments of t_1 were acquired, each with 352 scans and 4 s recycle delay. The sweep widths in the f_1 and f_2 dimensions were 1400 and 700 Hz, respectively, and the echo delay time during double quantum preparation period was 18 ms. The indicated peak assignments were determined from the observed correlations using a peak assignment algorithm.²⁵

the peaks broaden substantially such that the resolution of the individual Si sites is lost. This line broadening can be attributed to a relaxation effect (the ^{29}Si T_2 relaxation times become short as the temperature is lowered) arising from paramagnetic molecular oxygen present in the cavities of the zeolite in addition to the sorbate molecules.²² In the present work, although data were collected in the temperature range of 265–295 K, only the data obtained at 280 K are presented in detail here.

Peak Assignment. The first step toward locating guest molecules in zeolites by this solid-state NMR method involves assigning the peaks in the ^{29}Si spectrum. To assign the peaks in the ^{29}Si MAS NMR spectra to the 12 unique Si sites in the zeolite framework, a 2D ^{29}Si INADEQUATE experiment^{23,24} was performed (Figure 2). The peaks were assigned using an algorithm which efficiently finds all possible sets of peak assignments for which the observed correlations and known connectivities are in agreement²⁵ which yielded two possible sets of assignments that are consistent with the observed correlations in the INADEQUATE spectrum. The chosen assignment (indicated in Figure 2) gives a much stronger correlation between the ^{29}Si chemical shifts and structural parameters from the crystal structure⁴ (e.g. the mean Si–Si distances) and is consistent with the peak assignments obtained for similar systems (e.g. the *p*-xylene/ZSM-5 complex²⁴).

(22) Fyfe, C. A.; Brouwer, D. H. *J. Am. Chem. Soc.* **2004**, *126*, 1306.

(23) Bax, A.; Freeman, R.; Kempsell, S. P. *J. Am. Chem. Soc.* **1980**, *102*, 4849.

(24) Fyfe, C. A.; Grondy, H.; Feng, Y.; Kokotailo, G. T. *J. Am. Chem. Soc.* **1990**, *112*, 8812.

(25) Brouwer, D. H. *J. Magn. Reson.* **2003**, *164*, 10.

(21) Wolfram, S., *Mathematica: A System for Doing Mathematics by Computer*; v. 3.0, Wolfram Media: Champaign IL, 1996.

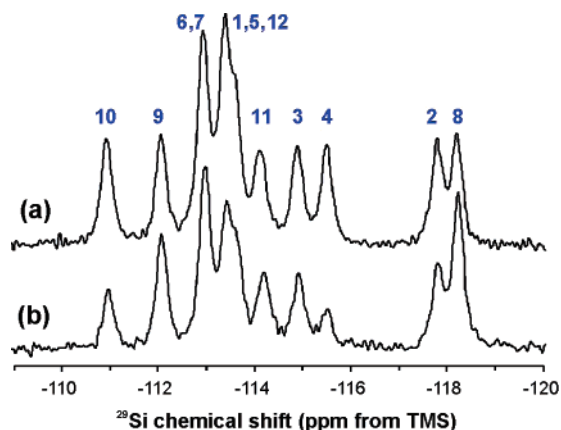


Figure 3. Comparison of the (a) quantitative ^{29}Si MAS and (b) $^1\text{H}/^{29}\text{Si}$ CP MAS spectra of the low-loaded pDCB/ZSM-5 complex at 280 K. Note that the intensities of a number of the Si peaks (Si8 and Si9) are enhanced compared to the others. The quantitative spectrum was acquired with 32 scans and a 30 s recycle delay. The CP spectrum was acquired with 640 scans, a contact time of 15 ms, and a recycle delay of 2 s. ^1H decoupling was not applied during acquisition for either spectrum.

Polarization Transfer Experiments. With the individual peaks in the ^{29}Si spectrum assigned, it is possible to proceed to the determination of the location of the guest molecules in the zeolite framework. The $^1\text{H}/^{29}\text{Si}$ CP MAS NMR experiment provides information about ^1H – ^{29}Si internuclear distances, since the rate of magnetization transfer between ^1H and ^{29}Si nuclei depends on the strength of the ^1H – ^{29}Si dipolar couplings. Qualitatively, the intensity of a peak in a $^1\text{H}/^{29}\text{Si}$ CP MAS NMR spectrum will reflect how close the Si site is to the protons of the guest molecule. Figure 3 compares a quantitative ^{29}Si spectrum to a $^1\text{H}/^{29}\text{Si}$ CP MAS spectrum. The relative intensities of the peaks in the CP spectrum show a definite discrimination and indicate that the ^1H nuclei of the pDCB molecule are close to Si8 and Si9, quite far away from Si4 and Si10, and at a medium distance from the other Si sites. This qualitative analysis indicates that the molecules are likely located somewhere in the straight channels or channel intersections and not in the zigzag channels. We now consider how the rates of magnetization transfer in $^1\text{H}/^{29}\text{Si}$ CP experiments can best be measured experimentally and used in a quantitative manner to determine the exact locations of the guest molecules in the zeolite framework.

In a previous paper,¹⁸ we described and discussed the measurement of $^1\text{H}/^{29}\text{Si}$ CP rate constants in zeolite–sorbate complexes in depth, and only the main points are summarized here. The rate of $^1\text{H}/^{29}\text{Si}$ cross polarization can be measured by performing a variable contact time $^1\text{H}/^{29}\text{Si}$ CP MAS experiment and plotting the ^{29}Si peak areas as functions of the contact time. The contact time dependence of the S spin magnetization during $I \rightarrow S$ cross polarization (where the I spin are abundant and the S spins are rare) is described by the following expression

$$S_{\text{CP}}(t) = I_0 \frac{k_{IS}}{(k_{IS} + k_S) - k_I} \{ \exp(-k_I t) - [\exp(-(k_{IS} + k_S)t)] \} \quad (1)$$

where k_I and k_S are the rate constants for spin-lock relaxation ($T_{1\rho}$) of the I and S spins respectively, k_{IS} is the rate of cross polarization between the I and S spins, and I_0 reflects the initial magnetization of the I spins. For most systems, the increase in

the S spin magnetization is governed by the rate constant k_{IS} (assuming k_S is small), and its decay is governed by k_I , the $T_{1\rho}$ relaxation of the I spins. This normal situation is termed the “fast CP regime.” As Klur et al. have pointed out,²⁶ when the rate of I spin-lock relaxation is fast compared to the rate of $I \rightarrow S$ cross polarization ($k_I > k_{IS}$), the dynamics of the S spin magnetization in the CP curve is reversed from the usual assumptions: the rate of growth of the S spin magnetization is governed by k_I while its decay is governed by $k_{IS} + k_S$. This situation is termed the “slow CP regime.”

Due to the presence of paramagnetic oxygen in the cavities of the zeolite–sorbate complexes,²² ^1H and ^{29}Si spin-lock relaxation can occur quite rapidly, whereas the rate of $^1\text{H}/^{29}\text{Si}$ cross polarization can be slow since the dipolar interactions between the ^1H nuclei of the sorbate molecules and the ^{29}Si nuclei of the zeolite framework are quite weak and can be further averaged by motions of the guest molecules. It is important to recognize the slow CP regime for the measured CP rate constants to be correct, as an analysis assuming normal fast CP may lead to erroneous measurements. However, even when the slow CP regime is recognized, it is difficult to obtain absolute values for the CP rate constants from fits to standard CP curves since k_{IS} is highly correlated to I_0 and the contribution from ^{29}Si $T_{1\rho}$ relaxation (k_S) is ignored, and because it is difficult to obtain reliable data at very long contact times. We therefore investigated the use of the $^1\text{H}/^{29}\text{Si}$ CP “drain” or “depolarization” experiment^{27,28} to measure absolute CP rate constants in these systems.¹⁸

The dynamics of the S spin magnetization during a cross-polarization drain experiment are described by an exponential decay:

$$S(t) = S(0) \exp[-(k_S + k_{IS})t] \quad (2)$$

where $S(0)$ is the initial magnetization of the S spins. The exponential decay resulting from the CP drain experiment without the contact pulse applied on the I spins (“reference” experiment, S_0) is due entirely to S spin $T_{1\rho}$ relaxation and has the rate constant k_S since $k_{IS} = 0$. The exponential decay resulting from the CP drain experiment with the contact pulse applied on the I spins (“drain” experiment, S_d) has the rate constant $k_{IS} + k_S$. The analysis of the CP drain dynamics can be simplified by plotting the data as a normalized difference plot²⁸ ($\Delta S/S_0$, where $\Delta S = S_0 - S_d$) such that the CP rate constant is the only variable in the fit to the data:

$$\frac{\Delta S}{S_0} = 1 - \exp(-k_{IS}t) \quad (3)$$

Absolute values for the CP rates are thus obtained from these normalized CP drain curves, since the contributions from I_0 and both I and S $T_{1\rho}$ relaxation are removed.

A series of variable contact time $^1\text{H}/^{29}\text{Si}$ CP and CP drain experiments were carried out on the low-loaded pDCB/ZSM-5 complex at 280 K. The intensities for each Si peak were extracted, using peak positions and widths determined from the quantitative ^{29}Si spectra, and plotted as functions of the contact time as shown in Figures 4 and 5 for the CP and CP drain

(26) Klur, I.; Jacquinot, J.-F.; Brunet, F.; Charpentier, T.; Virlet, J.; Schneider, C.; Tekely, P. *J. Phys. Chem. B* **2000**, *104*, 10162.

(27) Schaefer, J.; McKay, R. A.; Stejskal, E. O. *J. Magn. Reson.* **1979**, *34*, 443.

(28) Stejskal, E. O.; Schaefer, J.; McKay, R. A. *J. Magn. Reson.* **1984**, *57*, 471.

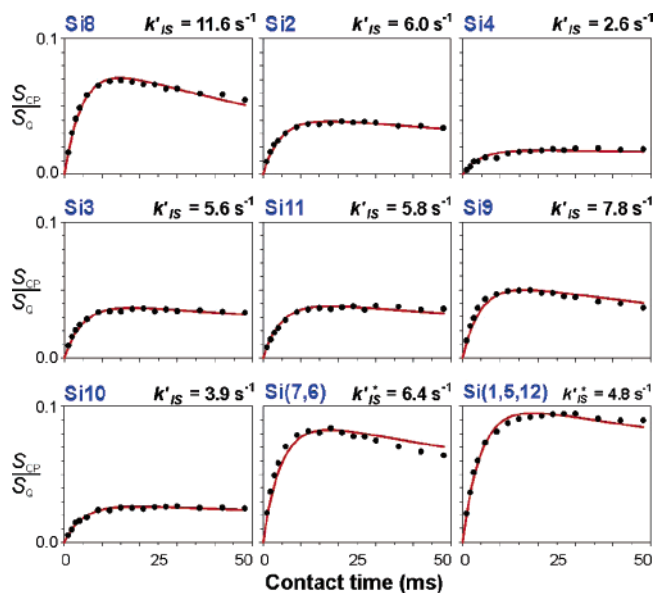


Figure 4. $^1\text{H}/^{29}\text{Si}$ cross polarization curves for the low-loaded pDCB/ZSM-5 complex at 280 K. The CP signal intensities are scaled with respect to a quantitative ^{29}Si MAS NMR spectrum, giving an indication of the absolute efficiency of the experiment. The curves were fit to eq 1 using the relative CP rate constants indicated in each graph with $I_0 = 1.5$, $k_I = 206 \text{ s}^{-1}$ ($^1\text{H } T_{1\rho} = 4.8 \text{ ms}$), and $k_S = 0 \text{ s}^{-1}$. At each contact time, 640 scans were collected with a 2 s recycle delay. For curves corresponding to groups of overlapping peaks, the fitted CP rate constants are considered to be an average and are denoted by an asterisk (k'_{IS^*}).

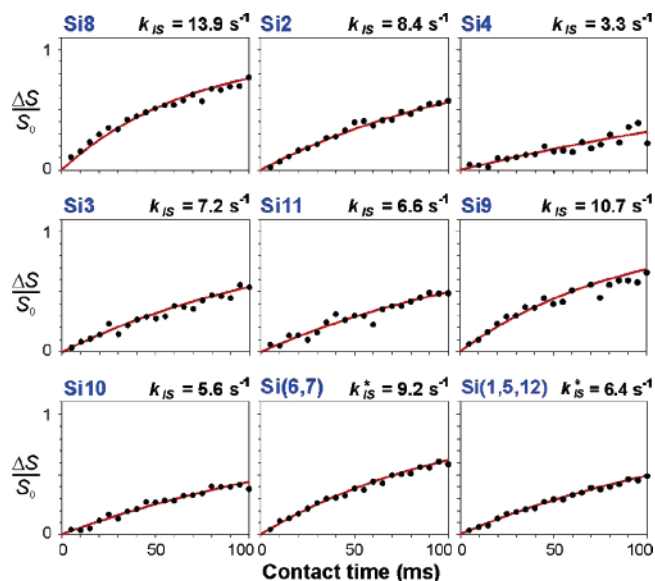


Figure 5. Normalized $^1\text{H}/^{29}\text{Si}$ cross polarization drain difference curves ($\Delta S/S_0$) for the low-loaded pDCB/ZSM-5 complex at 280 K. The curves were fit to eq 3 using the CP rate constants indicated in each graph. At each contact time, reference and drain spectra were acquired with 24 scans and a 25 s recycle delay. For curves corresponding to groups of overlapping peaks, the fitted CP rate constants are considered to be an average and are denoted by an asterisk (k_{IS^*}).

experiments, respectively. The intensities of the signals in the $^1\text{H}/^{29}\text{Si}$ CP spectra were very low compared to the quantitative spectrum, indicating that the CP process is very inefficient, a characteristic of the slow CP regime. The CP rate constants for each Si peak were therefore extracted from the CP curves presented in Figure 4 by fitting the data to eq 1, assuming the spin dynamics were in the slow CP regime, neglecting the contribution for the $^{29}\text{Si } T_{1\rho}$ relaxation ($k_S = 0$), and using

identical values of I_0 and k_I for all CP curves. The success of the fitting using these assumptions is confirmation of the assumed model. Because the fitting parameters are highly correlated,¹⁸ the CP rate constants obtained from the CP curves are considered to be *relative* values and are denoted by k'_{IS} . Absolute values for the CP rate constants (k_{IS}) were obtained by fitting the CP drain curves presented in Figure 5 to eq 3. Although the values for the rate constants obtained from the CP and CP drain experiments are somewhat different, it is important to note that the relative ordering of the different rate constants is the same in both experiments, and both ultimately yield the same structure as will be described below.

All of the parameters used to fit the ^{29}Si spectra, along with ^{29}Si relaxation times and $^1\text{H}/^{29}\text{Si}$ CP rate constants for the data collected at 280 K, are presented in Table 1. In the next step, these measured rates of cross polarization are related to the ^1H – ^{29}Si dipolar coupling strengths to determine the location of the sorbate molecule with respect to the Si sites in the zeolite framework.

2. Structure Determination

Outline of Strategy. The basis of the strategy to determine the locations of organic guest molecules in host zeolite frameworks from $^1\text{H}/^{29}\text{Si}$ cross polarization experiments is the relationship between the measured CP rate constants and the H–Si internuclear distances. The rates of cross polarization are proportional to the heteronuclear second moments (M_2^{IS}) of the dipolar line shapes since²⁹

$$k_{IS} = C \frac{M_2^{IS}}{\sqrt{M_2^I}} \quad (4)$$

where C is a constant and M_2^I , the I spin homonuclear second moment, is also a constant for the spin system. If both the I and S nuclei are spin- $1/2$, the heteronuclear second moment for a powder, referred hereafter to as simply M_2 , can be calculated according to Van Vleck³⁰ as a pairwise summation of the inverse sixth powers of the I – S internuclear distances (in units of Hz^2):

$$M_2 = \left(\frac{1}{2\pi}\right)^2 4 \left(\frac{1}{5} \frac{\gamma_I \gamma_S \hbar \mu_0}{4\pi r_{IS}}\right)^2 \sum \frac{1}{r_{IS}^6} \quad (5)$$

assuming that the structure is rigid. Hence,

$$k_{IS} \propto M_2 \propto \sum r^{-6} \quad (6)$$

The strategy for determining the guest molecule locations in host zeolite frameworks is essentially to find all possible locations of the guest molecules for which the proportionality between the set of *experimental* $^1\text{H}/^{29}\text{Si}$ CP rate constants and the set of heteronuclear second moments *calculated* from the H–Si distances (eq 6) is satisfied.¹³ The algorithm which has been developed for this purpose is described in detail in the following using the $^1\text{H}/^{29}\text{Si}$ CP drain data for the low-loaded pDCB/ZSM-5 complex collected at 280 K as a working example.

The location of rigid guest molecules, such as *p*-disubstituted aromatics, in the zeolite can be defined by six parameters, three

(29) Pines, A.; Gibby, G.; Waugh, J. S. *J. Chem. Phys.* **1973**, *59*, 569.

(30) van Vleck, J. H. *Phys. Rev.* **1948**, *74*, 1168.

Table 1. Experimental and Calculated Parameters Related to the $^1\text{H}/^{29}\text{Si}$ Cross Polarization Experiments for the Low-Loaded pDCB/ZSM-5 Complex at 280 K

Si site	spectrum parameters ^a		relaxation times ^b			CP rate constants ^c		second moment ^d (10^3 Hz^2)
	shift (ppm)	width (Hz)	T_1 (s)	T_2 (ms)	$T_{1\rho}$ (ms)	k_{IS} (s^{-1})	k'_{IS} (s^{-1})	
8	-118.2	18.5	5.2 ± 0.2	20 ± 2	223 ± 9	13.9 ± 0.3	11.6 ± 0.1	108.7
2	-117.8	19.8	2.1 ± 0.1	19 ± 1	113 ± 2	8.4 ± 0.1	6.0 ± 0.1	54.6
4	-115.5	19.8	1.7 ± 0.1	20 ± 2	100 ± 2	3.3 ± 0.2	2.6 ± 0.1	7.7
3	-114.9	20.3	1.8 ± 0.1	16 ± 1	108 ± 3	7.2 ± 0.2	5.6 ± 0.1	34.5
11	-114.1	22.8	6.6 ± 0.4	24 ± 2	271 ± 20	6.6 ± 0.2	5.8 ± 0.1	32.3
9	-112.1	18.1	1.8 ± 0.1	15 ± 1	94 ± 2	10.7 ± 0.3	7.8 ± 0.1	69.0
10	-110.9	18.2	2.4 ± 0.1	26 ± 1	132 ± 2	5.6 ± 0.1	3.9 ± 0.1	19.8
12	-113.6	17.6	2.6 ± 0.1	21 ± 1	130 ± 2	6.4 ± 0.1	4.8 ± 0.1	30.6
1	-113.4							54.7
5	-113.3							16.9
7	-113.0	17.6	2.0 ± 0.1	17 ± 1	97 ± 1	9.2 ± 0.1	6.4 ± 0.1	92.9
6	-112.9							21.2

^a Determined from a quantitative ^{29}Si MAS NMR spectrum. ^b Determined from ^{29}Si saturation recovery (T_1), spin–echo (T_2), and spin-locking ($T_{1\rho}$) experiments. ^c Determined from $^1\text{H}/^{29}\text{Si}$ CP drain (k_{IS}) and standard CP (k'_{IS}) experiments. ^d Calculated assuming a rigid lattice structure for the average location determined from the CP drain data (see Figure 9).

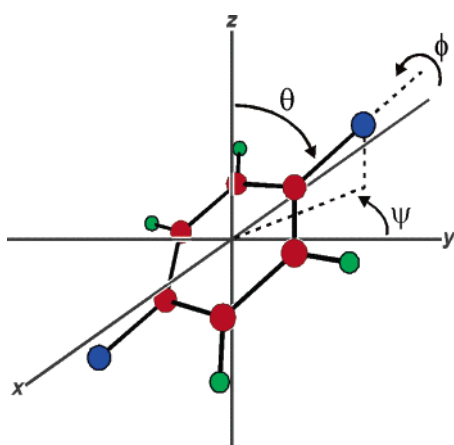


Figure 6. Definition of the orientation of the molecule in terms of the Euler rotation angles: ϕ represents rotation about the molecular long axis, whereas θ and ψ describe the orientation of the molecular long axis with respect to the crystallographic axes (assuming the molecule starts with its plane in the xz plane with the long axis along z and ring center at the origin).

parameters describing the translational position of the center of the molecule (x , y , z) and three Euler angles describing the rotational orientation (ϕ , θ , ψ). To place the molecule at a specified location, the molecule is first rotated according to the Euler angles and then translated. The rotation involves first rotating the molecule by an angle ϕ about the z axis, followed by a rotation of an angle θ about the x axis, and then rotation about the z axis again by an angle ψ . These rotations are applied about the crystallographic Cartesian axes (i.e. in the coordinate system of the zeolite framework). If the plane of the molecule is originally in the xz -plane centered at the origin with its long axis in the z direction, then θ and ψ denote the orientation of the molecule's long axis with respect to the z and y axes, respectively, and ϕ represents the rotation of the molecule about its long axis, as depicted in Figure 6. The pDCB molecule was assumed to have C–C, C–H, and C–Cl bond lengths of 1.39, 1.00, and 1.75 Å respectively and bond angles of 120°.

The zeolite framework is described by unit cell constants, symmetry operators of the space group, and the fractional atomic coordinates of the Si and O atoms. The zeolite framework for this working example was taken from the single-crystal XRD structure of the low-loaded pDCB/ZSM-5 complex.⁴ However,

to investigate the necessity of having the exact structure of the zeolite framework on the determined guest molecule location, the framework coordinates from the high-temperature (orthorhombic) single-crystal structure of the calcined (empty) ZSM-5 framework³¹ were also used in separate structure determinations.

Selection of Acceptable Solutions. A proposed location of the guest molecule in the zeolite framework is considered to be in agreement with the experimental NMR data if the following three criteria are met: (1) the location is physically reasonable (no unacceptably short host–guest interatomic distances), (2) there exists a high degree of linear correlation between the set of *experimental* CP rate constants and the set of *calculated* heteronuclear second moments, and (3) the predicted intensities for the groups of overlapping peaks are in agreement with the intensities obtained from the CP or CP drain experiments.

For this particular calculation, an initial test revealed that high degrees of linear correlation between k_{IS} and M_2 only existed for locations near the intersection of the straight and zigzag channels. Consequently, this region was investigated in detail with approximately 4×10^6 locations of the pDCB molecules tested within the following ranges: translations of $0.45 \leq x \leq 0.55$, $0.15 \leq y \leq 0.25$, and $-0.075 \leq z \leq 0.03$ (fractional coordinates) in steps of 0.2 Å and rotations of $20^\circ \leq \phi \leq 60^\circ$, $50^\circ \leq \theta \leq 130^\circ$, and $-40^\circ \leq \psi \leq 40^\circ$ in steps of 3° (ϕ) or 5° (θ and ψ). For simplicity, the degree symbol will be dropped in subsequent references to the Euler angles.

All of the proposed locations were first tested to ensure that they were physically reasonable. A location was considered to be unreasonable if any atoms of the guest molecule were too close to any Si or O atoms of the zeolite framework, as defined by a minimum guest–host distance ($d_{\min} = 2 \text{ Å}$ is a reasonable limit for zeolite–sorbate structures). For this particular structure calculation, the number of possible locations was reduced from 4×10^6 to 1.4×10^6 .

For each remaining physically reasonable location, the $^1\text{H}/^{29}\text{Si}$ second moments were calculated for each unique Si site, and the correlation between these calculated values and the experimental CP rates was tested for linearity. This involved a number of steps: (1) The molecule was moved to the location,

(31) van Koningsveld, H. *Acta Crystallogr.* **1990**, *B46*, 731.

specified by $\{x, y, z, \phi, \theta, \psi\}$, that was being tested. (2) All of the symmetry-equivalent locations were then generated by converting the molecule's coordinates from Cartesian into fractional coordinates, applying the symmetry operators for the particular space group, and then converting all atoms back into Cartesian coordinates. (3) For each unique Si site, all of the H atoms within a specified radius (8 Å in this calculation) were selected and used to calculate the heteronuclear second moment for each Si site according to eq 5. (4) For all of those Si sites which gave resolved peaks in the ^{29}Si spectrum, the degree of linear correlation (in the form of the r^2 value) between the experimental CP rate constants and the calculated second moments was determined. (5) The possible locations of the guest molecule were then selected by choosing only those locations which gave a degree of linear correlation between M_2 and k_{IS} above a specified minimum r^2 value. At this stage, the number of possible locations of the pDCB molecules in ZSM-5 which were consistent with the $^1\text{H}/^{29}\text{Si}$ CP rate constants obtained from the CP drain experiments at 280 K was dramatically reduced to 4013, 1807, or 526 when the minimum r^2 value was specified to be 0.96, 0.97, or 0.98, respectively.

In most cases, not all of the Si sites will give resolved peaks in the ^{29}Si spectrum, and there may be one or more peaks due to several Si sites with similar or identical chemical shifts. The intensities of these groups of overlapping peaks in the $^1\text{H}/^{29}\text{Si}$ CP or CP drain spectra can be used for a further testing of the locations selected by the r^2 value in the previous step. For each location, the CP rate constants for the Si sites that give overlapping peaks can be predicted using the linear correlation between k_{IS} and M_2 previously found for the resolved Si sites. These calculated k_{IS} values can then be inserted into eq 1 or eq 2 to predict the intensities of the overlapping peaks in the CP or CP drain spectra. These predicted intensities have to be in good agreement with the experimentally observed intensities for the location to be considered acceptable.

In the ^{29}Si spectrum of the low-loaded pDCB/ZSM-5 complex at 280 K (Figure 3) there are seven resolved peaks and two groups of overlapping peaks. As an example, consider the location $\{x = 0.490, y = 0.210, z = -0.030, \phi = 45, \theta = 90, \psi = 5\}$ that gives the following linear correlation based on the measured k_{IS} (from the CP drain data) and M_2 values calculated for the Si sites with resolved peaks:

$$\hat{k}_{IS} = 3.10 + [(1.09 \times 10^{-4})M_2] \quad (7)$$

with $r^2 = 0.987$ and a standard deviation of regression (SDR) of 0.440 where

$$\text{SDR} = \sqrt{\frac{\sum_i^n (k_{IS}^i - \hat{k}_{IS}^i)^2}{n - 2}} \quad (8)$$

and \hat{k}_{IS} denotes linear regression line and n denotes the number of resolved Si peaks for which CP rate constants were measured. At this particular location of the pDCB molecule, the heteronuclear second moments are calculated according to eq 5 to be 22 505 Hz² and 81 680 Hz² for sites Si6 and Si7, respectively. With the linear correlation in eq 7, these M_2 values predict the CP rate constants for Si6 and Si7 to be 5.55 ± 1.25 and 11.97 ± 1.32 respectively, where the errors represent the 95% (1 -

α , with $\alpha = 0.05$) prediction interval:³²

$$\hat{k}_{IS} \pm t(\alpha/2) \times \text{SDR} \times \sqrt{1 + \frac{1}{n} + \frac{(M_2 - \sum M_2^i/n)^2}{(\sum M_2^i) - (\sum M_2^i)^2/n}} \quad (9)$$

where $t(\alpha/2)$ is from the Student's t distribution (normal distribution)³² with $n - 2$ degrees of freedom. These predicted rate constants can then be put into the equations for a CP curve (eq 1) or CP drain decay (eq 2). For the $^1\text{H}/^{29}\text{Si}$ CP drain spectrum with a contact time of 100 ms, the normalized intensities for Si6 and Si7 are predicted to be 0.42 ± 0.07 and 0.70 ± 0.04 respectively, and thus the normalized intensity of this group of overlapping peaks is predicted to be the average, 0.56 ± 0.06 . Since the experimental normalized intensity for the Si(6,7) peak is 0.59 and falls within the prediction interval (as does the intensity for the Si(1,5,12) peak), this location of the molecule is accepted. In this manner, all groups of overlapping peaks for each location were tested against the CP or CP drain spectra and the number of acceptable solutions further reduced. For this working example, the number of solutions were reduced at this stage from 4013 to 3446, 1807 to 1534, and 526 to 431 for the minimum r^2 values of 0.96, 0.97, and 0.98 respectively.

Display and Summary of Solutions. At the end of these calculations, there may be tens, hundreds, even thousands of locations which agree with the experimental cross polarization data within the specified errors, according to the criteria outlined above. It is therefore desirable to summarize and display these results in a meaningful and nonsubjective manner that will allow comparisons to be made between different structure determinations by NMR and with XRD data if available. One approach is to construct plots of the number of solutions for each value of $x, y, z, \phi, \theta,$ and ψ as shown in Figure 7 which give an idea of the distribution of the solutions for each parameter. By assuming that these distributions approximate the normal distribution, the large number of solutions can be summarized by taking the mean and standard deviations of each plot. In this manner, the "average" location of pDCB in ZSM-5 determined from the $^1\text{H}/^{29}\text{Si}$ CP drain data collected at 280 K is described by fractional coordinates of $\{x, y, z\} = \{0.488 \pm 0.005, 0.218 \pm 0.017, -0.023 \pm 0.008\}$ with a rotational orientation of $\{\phi, \theta, \psi\} = \{41 \pm 4, 93 \pm 12, 2 \pm 13\}$ based on the solutions with $r^2 \geq 0.98$.

In these plots in Figure 7, the effect of changing the specified minimum r^2 value can be seen. As the r^2 value is lowered, the number of acceptable solutions increases, and there is a larger distribution of solutions, as one would expect, yet the average location remains relatively unchanged. The plots also show that the greatest uncertainties in this particular structure determination are in y (translation along the channel) and θ and ψ (orientation of the molecule's long axis), whereas the molecule is very well defined with respect to the $x, z,$ and ϕ parameters. The distribution of the θ parameter is the only one that deviates significantly from a normal distribution. The bimodal nature of this distribution may suggest that the pDCB molecule is disordered over two closely related sites at the channel intersec-

(32) Chase, W.; Brown, F. *General Statistics*, 2nd ed.; John Wiley & Sons: New York, 1992.

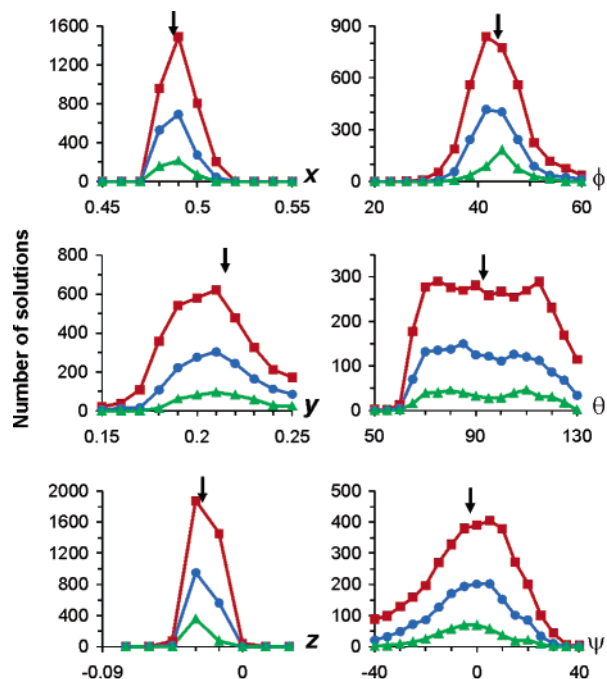


Figure 7. Distributions of the solutions for the location of pDCB in ZSM-5 from $^1\text{H}/^{29}\text{Si}$ CP drain data collected at 280 with linear correlations of $r^2 \geq 0.96$ (red squares), $r^2 \geq 0.97$ (blue circles), and $r^2 \geq 0.98$ (green triangles). The arrows indicate the average location of all the solutions with $r^2 \geq 0.98$: $\{x = 0.488 \pm 0.007, y = 0.213 \pm 0.017, z = -0.027 \pm 0.006, \phi = 45 \pm 4, \theta = 94 \pm 17, \psi = -3 \pm 13\}$.

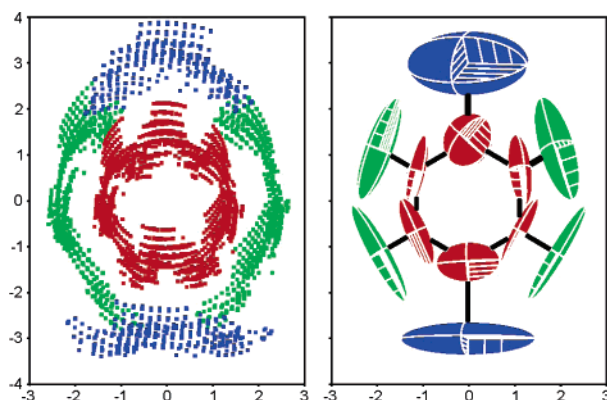


Figure 8. (a) Scatter plot of the guest molecule atomic positions for all solutions with $r^2 \geq 0.98$ determined from the $^1\text{H}/^{29}\text{Si}$ CP drain data at 280 K. (b) Average location of solutions with $r^2 \geq 0.98$ along with 50% error ellipsoids which represent the distribution of solutions. Both plots are viewed in the plane of the molecule with the axes in units of Å. The vertical axis is coincident with the crystallographic b axis (H – green, C – red, Cl – blue).

tion. Alternatively, the distribution may reflect the insensitivity of the structure determination method to this parameter.

A second approach to summarizing the large number of solutions from which the definition of the structure can be visually evaluated and which can be compared directly with XRD structural data is to determine error estimates for the positions of the atoms of the guest molecule. Figure 8a displays a scatter plot of all the atomic positions for each atom for all the solutions with $r^2 \geq 0.98$ which visually displays the distribution of the solutions. This scatter in the location of each atom can be represented by an error ellipsoid in which the length of each principal axis is proportional to the root-mean square distance from the mean position (see Supporting Information).

Figure 8b shows that these ellipsoids represent the error in the corresponding scatter plots quite well. The error ellipsoids can be expressed in the same form as the anisotropic displacement parameters used in crystallography to model small atomic motions and thus are easily displayed by crystallography graphics programs such as ORTEP.³³ It is important to note that the error ellipsoids presented here do not have a very well-defined physical meaning (unlike the atomic displacement parameters used in crystallography) other than giving a relatively simple graphical description of the scatter among the many possible locations of a guest molecule found by this solid-state NMR technique. It is also very important to note that all of the atomic positions are determined entirely by the H positions since only these are determined by this analysis, unlike the situation in XRD where the scattering is from electrons with all atoms contributing to different degrees.

Figure 9 displays this average location of the pDCB molecule in the zeolite framework, together with the error ellipsoids. The set of atomic coordinates and error ellipsoid parameters are provided in the Supporting Information. This gives a clear picture of where the molecule is located, as well as an idea of the distribution of the large number of solutions that agree with the experimental data within the chosen fit criteria. The error ellipsoids illustrate the greater uncertainty in the position along the straight channel axis (y -direction) and in the orientation of the long axis (θ and ψ). This location determined by solid-state NMR spectroscopy is in excellent agreement with the structure determined from single-crystal XRD data.⁴ The pDCB molecules were located correctly in the channel intersection with the correct rotational orientation (see Figure 9).

Figure 10 displays the linear correlation between the experimental CP rate constants (k_{IS}) and the calculated heteronuclear second moments (M_2) for the average of the solutions with $r^2 \geq 0.98$. This linear correlation can then be used to predict all the CP rate constants from which the entire CP or CP drain spectrum can be predicted using the calculated peak intensities (according to eq 1 or eq 2) and the peak positions and widths fit from the quantitative spectrum (Table 1). Figure 11 shows the excellent agreement between the experimental and predicted spectra for the CP drain difference spectrum (100 ms contact time). This final test confirms that the guest molecule location is fully consistent with all the available experimental $^1\text{H}/^{29}\text{Si}$ cross polarization drain data.

3. Reliability and Robustness of Method

In the example described above, in which the location of pDCB in ZSM-5 determined by this solid-state $^1\text{H}/^{29}\text{Si}$ CP MAS NMR technique was found to be in excellent agreement with the single-crystal XRD structure, the structure determination was performed under somewhat ideal conditions since the CP rate constants used were reliable in absolute terms (obtained from fits to the CP drain curves) and the zeolite framework coordinates used were from the single-crystal XRD structure for the pDCB/ZSM-5 complex. In the following, we now demonstrate that the algorithm is very robust, since essentially the same location for the pDCB molecule is found using relative CP rate constants and under a variety of possibly complicating

(33) Burnett, M. N.; Johnson, C. K. *ORTEP-III*; Oak Ridge Thermal Ellipsoid Plot Program for Crystal Structure Illustrations; Oak Ridge National Laboratory, Tennessee, Report ORNL-6895, 1996.

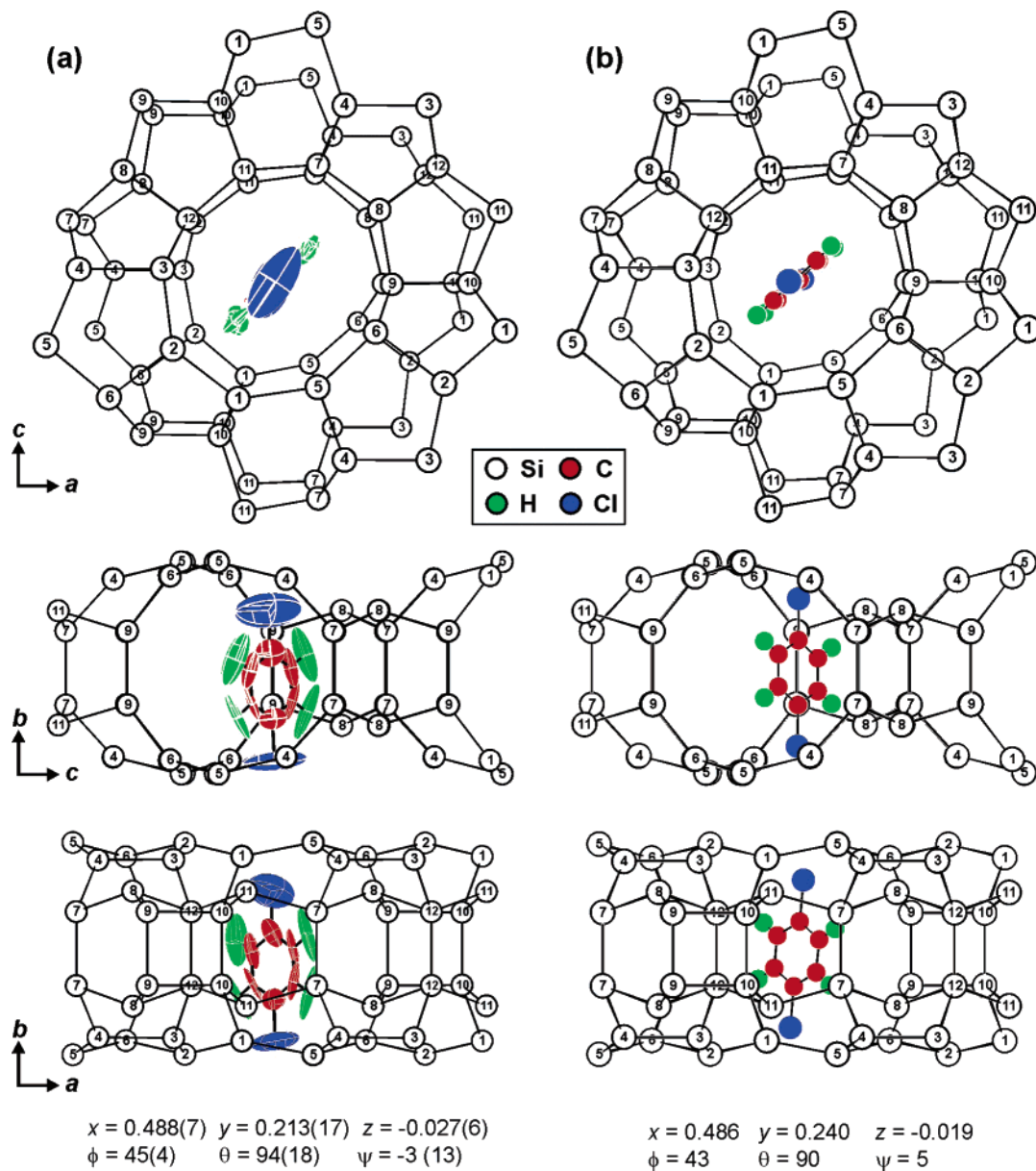


Figure 9. (a) Average location (with 50% error ellipsoids) of the pDCB molecule in ZSM-5 for solutions with $r^2 \geq 0.98$ from the $^1\text{H}/^{29}\text{Si}$ CP drain data collected at 280 K. (b) Location of *p*-dichlorobenzene molecule determined by single-crystal XRD:⁴ view down the straight channels (*top*), view down the zigzag channels (*middle*), view perpendicular to straight and zigzag channels (*bottom*).

factors such as using zeolite framework coordinates that only approximate those found for exactly this complex and over a range of temperatures.

Use of Relative CP Rate Constants. The CP rate constants obtained from the standard $^1\text{H}/^{29}\text{Si}$ CP curves (k'_{IS}) can only be considered as relative values since they are highly correlated to the other fitting parameters (I_0 and k_i) and the contributions from the ^{29}Si $T_{1\rho}$ relaxation are ignored.¹⁸ However, since the algorithm searches for locations of the guest molecules which give a proportional relationship between the CP rate constants and second moments, it is not crucial that absolute values of the rate constants be used, and the relative CP rate constants obtained from standard $^1\text{H}/^{29}\text{Si}$ CP experiments can still be used to reliably determine the location of the guest molecule in the host zeolite framework.

The rate constants determined from the $^1\text{H}/^{29}\text{Si}$ CP curves collected at 280 K (see Figure 4) were used as input for the

structure determination algorithm, and the calculations were carried out in exactly the same manner as described above for the CP drain data. There were 93 solutions which were physically reasonable, had strong linear correlations ($r^2 > 0.98$) between these experimental rate constants and the calculated second moments, and gave good agreement between experimental and predicted intensities of the groups of overlapping peaks. The average of these locations is described by the fractional coordinates $\{x, y, z\} = \{0.491 \pm 0.007, 0.193 \pm 0.015, -0.011 \pm 0.009\}$ and rotational orientation of $\{\phi, \theta, \psi\} = \{43 \pm 4, 91 \pm 8, 12 \pm 24\}$. This location is in good agreement with the location determined from the CP drain data and also with the single-crystal XRD structure. Figure 12 displays the linear correlation between the experimental CP rate constants (k'_{IS}) and the calculated heteronuclear second moments (M_2) for this average location. From this correlation, the entire $^1\text{H}/^{29}\text{Si}$ CP spectrum at a contact time of 15 ms was predicted.

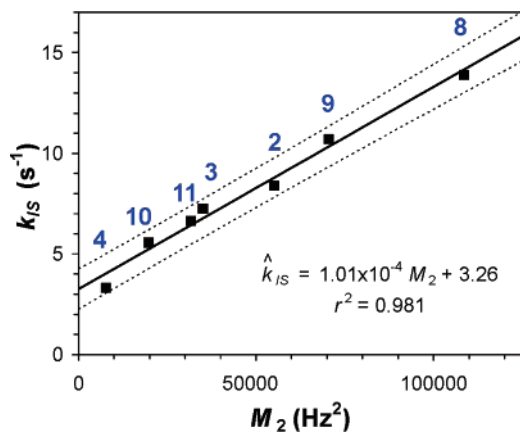


Figure 10. Plot of the experimentally determined CP rate constants (k_{IS}) from the CP drain experiment against the calculated heteronuclear second moments (M_2) for the average position of pDCB in ZSM-5 with $r^2 \geq 0.98$ from the $^1\text{H}/^{29}\text{Si}$ CP drain data collected at 280 K. The solid line is the line of best fit and the dashed lines represent the 95% confidence prediction interval (eq 9).

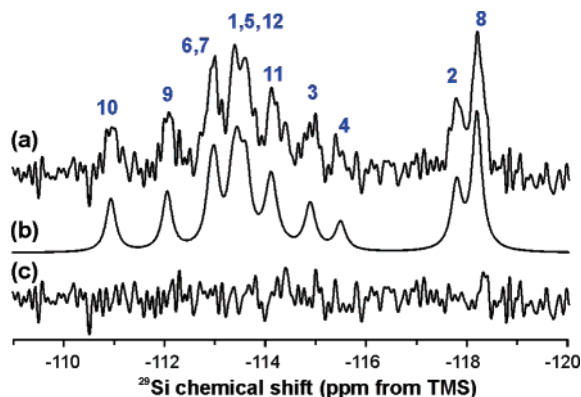


Figure 11. Comparison of experimental and predicted spectra for the average location of pDCB in ZSM-5 with $r^2 \geq 0.98$ determined from the $^1\text{H}/^{29}\text{Si}$ CP drain data collected at 280 K. (a) Difference spectrum between the CP drain “reference” (S_0) and “drain” (S_d) spectra at a contact time of 100 ms. (b) Predicted spectrum using the linear relationship between k_{IS} and M_2 in Figure 10. (c) Difference between experimental and predicted spectra.

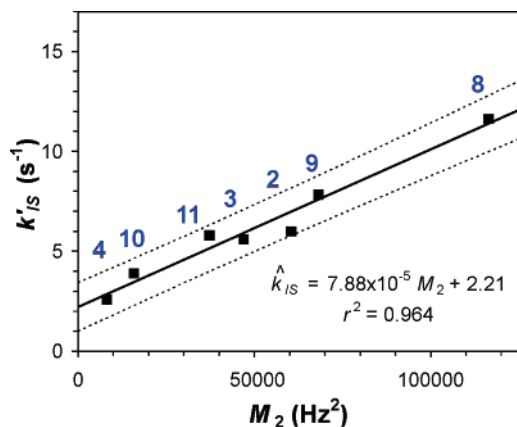


Figure 12. Plot of the experimentally determined CP rate constants (k'_{IS}) from CP curve fitting versus the calculated heteronuclear second moments (M_2) for the average position of pDCB in ZSM-5 with $r^2 \geq 0.98$ from the $^1\text{H}/^{29}\text{Si}$ CP data collected at 280 K. The solid line is the line of best fit, and the dashed lines represent the 95% confidence prediction interval (eq 9).

Figure 13 shows the excellent agreement between the experimental and predicted CP spectra, confirming that this location is consistent with the $^1\text{H}/^{29}\text{Si}$ CP MAS NMR data. A full

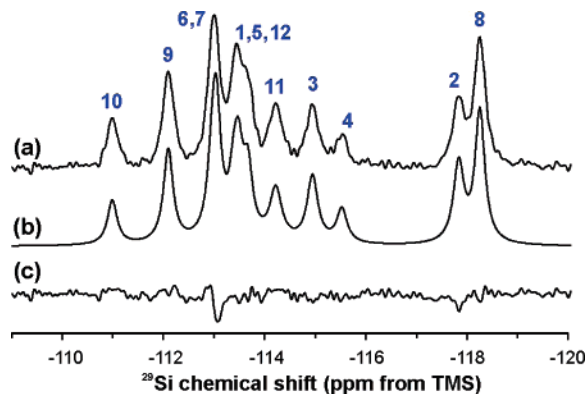


Figure 13. Comparison of experimental and predicted spectra for the average location of pDCB in ZSM-5 with $r^2 \geq 0.98$ determined from the $^1\text{H}/^{29}\text{Si}$ CP data collected at 280 K. (a) Experimental $^1\text{H}/^{29}\text{Si}$ CP MAS NMR spectrum at a contact time of 15 ms, (b) predicted spectrum using the linear relationship between k'_{IS} and M_2 in Figure 12, (c) difference between experimental and predicted spectra.

comparison of the locations determined from $^1\text{H}/^{29}\text{Si}$ CP and CP drain data is given in Figure 14.

Sensitivity to Exact Zeolite Framework Coordinates. A very reasonable concern is that this approach to locate the guest molecules may be sensitive to the exact zeolite framework coordinates used. It is known that the ZSM-5 framework is somewhat flexible, in that it interacts strongly with sorbed organic molecules and distorts to accommodate the guest molecules.^{19,34–36} For example, when pDCB (or any similar sorbate) is sorbed into ZSM-5, the framework undergoes a phase change from monoclinic to orthorhombic symmetry and the 10-ring pore openings distort from being circular to elliptical.⁴ It is known that the success of theoretical energy minimization approaches to structure determinations on these systems is very dependent on having the exact framework coordinates for exactly this complex being studied.³⁷

In the present work, to this point, the zeolite framework coordinates used in the structure determinations thus far have been those determined by van Koningsveld et al. from a single crystal of ZSM-5 loaded with 2.56 molecules of *p*-dichlorobenzene which includes these distortions.⁴ The concern arises when this structure determination protocol is applied to a completely unknown system in which the exact structure of the zeolite framework cannot be known from solid-state NMR and no diffraction-determined coordinates are available. In this situation, is it possible to assume a general framework topology and ignore any specific structural changes that the guest molecule may induce in the framework and still obtain the correct structure by NMR? To keep the present structural analysis as general as possible, we investigated the effect of the choice of zeolite framework coordinates used in these calculations on the end result.

The calculations to locate the pDCB molecule described above were repeated using both the experimental CP rate constants determined from the CP drain (Figure 5) and those from the standard CP (Figure 4) data collected at 280 K and a

(34) Fyfe, C. A.; Kennedy, G. J.; De Schutter, C. T.; Kokotailo, G. T. *J. Chem. Soc., Chem. Commun.* **1984**, 541.

(35) Fyfe, C. A.; Stobl, H.; Kokotailo, G.; Kennedy, G. J.; Barlow, G. E. *J. Am. Chem. Soc.* **1988**, *110*, 3373.

(36) Fyfe, C. A.; Strobl, H.; Gies, H.; Kokotailo, G. T. *Can. J. Chem.* **1988**, *66*, 1942.

(37) Snurr, R. Q.; Bell, A. T.; Theodorou, D. N. *J. Phys. Chem.* **1993**, *97*, 13742.

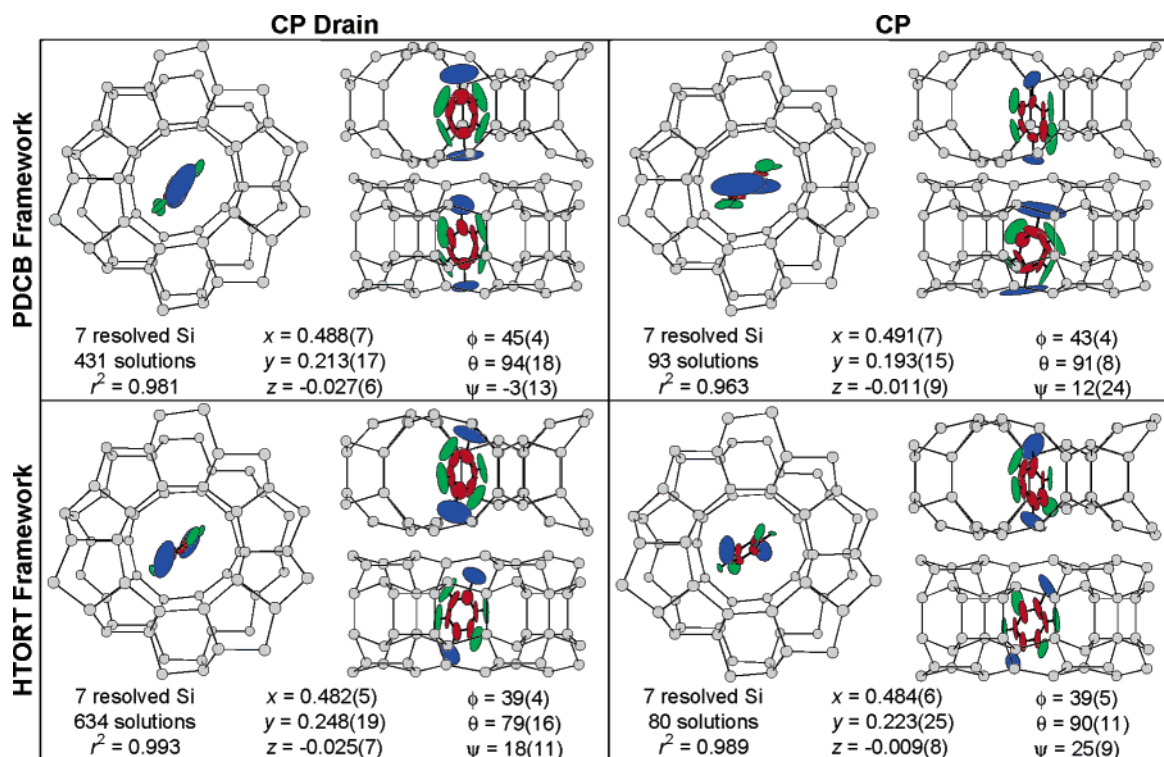


Figure 14. Comparison of the average locations (with 50% error ellipsoids) of pDCB in ZSM-5 determined from the $^1\text{H}/^{29}\text{Si}$ CP drain data (left) and standard CP data (right) obtained at 280 K using the ZSM-5 framework atomic coordinates from the pDCB/ZSM-5 crystal structure⁴ (upper) and from the empty HTORT crystal structure³¹ (lower). For each structure, the views are along the straight channel, *b* axis (left); along the zigzag channel, *a* axis (upper right); perpendicular to both the straight and zigzag channels, *c* axis (lower right). Below each structure is indicated the number of resolved ^{29}Si peaks used for the structure determination, the number of solutions with $r^2 \geq 0.98$, the parameters describing the position and orientation of the average of these solution (with standard deviations), and the r^2 value for the average location.

more general zeolite framework, that of the high-temperature orthorhombic phase of calcined (empty) ZSM-5³¹ (hereafter referred to as “HTORT”). This framework has circular pore openings, is not distorted by any template or sorbate molecules, and was obtained at elevated temperature (350 K). The average locations of the pDCB molecule from these different situations are presented in Figure 14 and are generally in good agreement with the location calculated using the same sets of CP rate constants and the framework coordinates from the pDCB/ZSM-5 crystal structure. The pDCB molecule was consistently located in the channel intersection, and the largest deviations seemed to be in the exact rotational orientation of the molecule. This probably arises from the fact that this technique is not very sensitive to θ and ψ (see the distributions in Figure 7) as the ^1H positions do not change a great deal under these rotations.

This consistency demonstrates that this solid-state NMR technique is robust enough to not require precise knowledge of the exact framework coordinates a priori. In contrast, theoretical energy minimization calculations (which use a rigid framework) are dependent on the exact structure of the framework³⁷ and can give incorrect answers if the correct framework structure is not available to be used. This is of critical practical importance as the exact framework structure will not usually be known. This difference between the techniques arises because the relative ^1H – ^{29}Si distances are only slightly affected by small changes in the atomic positions of the framework, whereas the nonbonding energies are very small compared to the large changes in energy that can be caused by small changes in the covalently bonded network of the zeolite framework.

Effect of Temperature and Motions. In all of the above structure determinations, the motions of the guest molecules in the zeolite cavities have been neglected, with the heteronuclear second moments being calculated by assuming a rigid structure. For similar complexes (e.g. *p*-xylene in ZSM-5¹³), it is known from ^2H NMR studies³⁸ that the guest molecules are at least undergoing 180° ring flips about the long molecular axis at a temperature of 280 K, with other motions not detectable by ^2H NMR likely to be occurring as well. It is possible that the motions of the guest molecules could lead to varying degrees of averaging of the $^1\text{H}/^{29}\text{Si}$ second moments for the different Si sites and therefore affect the linear correlation between k_{IS} and M_2 . Consequently, the effects of including various guest molecule motions in the calculation of the second moment have been investigated.

Four possible types of motions of the guest pDCB molecules in the ZSM-5 channel system were considered, listed in order of expected increasing energy barrier: (1) the molecule jumping between equivalent locations in each channel intersection that are related by mirror symmetry; (2) 180° ring flips about the long axis of the molecule; (3) translation from one channel intersection to another along the straight channel; (4) reorientation of the molecule (i.e. 180° flip perpendicular to long axis) and the second moments recalculated to take these motions into account.^{39–41} Specifically, using the approach described by Goc in refs 40 and 41 for calculating second moments in systems

(38) Kustanovich, I.; Fraenkel, D.; Luz, Z.; Vega, S.; Zimmermann, H. *J. Phys. Chem.* **1988**, *92*, 4134.

(39) Michel, J.; Drifford, M.; Rigney, P. *J. Chim. Phys.* **1970**, *67*, 31.

(40) Goc, R. *Solid State Nucl. Magn. Reson.* **1998**, *13*, 55.

(41) Goc, R. *J. Magn. Reson.* **1998**, *132*, 78.

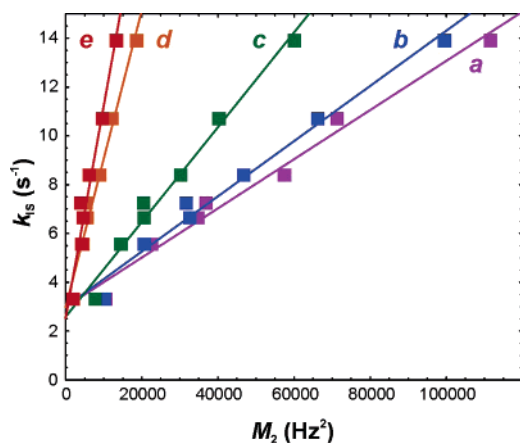


Figure 15. Plots of the correlations between CP rate constants (k_{IS}) and $^1\text{H}/^{29}\text{Si}$ second moments (M_2) with the calculations of the second moments taking into account the following motions of the pDCB guest molecules in the ZSM-5 channels: (a) no motion ($r^2 = 0.979$), (b) jumping between mirror-related sites in channel intersection ($r^2 = 0.981$), (c) 180° ring flipping about the long axis of the molecule ($r^2 = 0.981$), (d) translation between channel intersections along a straight channel ($r^2 = 0.970$), (e) reorientation, i.e. 180° flipping perpendicular to the long axis of the molecule ($r^2 = 0.956$).

with internal motions, the $^1\text{H}/^{29}\text{Si}$ second moments were calculated for each Si site, assuming these different types of motions using the NMR-determined location of pDCB from the CP drain experiments at 280 K (see Figure 9) and the Si framework coordinates from the pDCB single-crystal XRD structure.⁴ The calculations for the higher-energy motions included all of the lower-energy motions (e.g. the ring flipping also includes jumping between mirror-related sites in the channel intersection). A table of the calculated second moments under each level of motion is provided in the Supporting Information. The k_{IS} vs M_2 correlation plots (Figure 15) demonstrate that the degree of linear correlation between k_{IS} and M_2 changes very little under the different levels of motion, indicating that the motions affect the $^1\text{H}/^{29}\text{Si}$ second moments of the different Si sites to the same degree. This suggests that structure determinations in which these motions were accounted for in the calculation of the second moments would yield similar locations for the guest molecules. Therefore, this NMR structure determination method appears to be relatively insensitive to (well-defined) guest molecule motions, at least for the pDCB/ZSM-5 complex studied in this work at this temperature.

Structure determinations of the pDCB/ZSM-5 complex were also carried out using $^1\text{H}/^{29}\text{Si}$ CP MAS NMR data collected at 265 and 295 K (see Supporting Information), and the pDCB locations were found to be nearly identical to those determined at 280 K. A similar situation was previously found for the low-loaded complex of *p*-xylene, albeit at a lower temperature range.¹³ The effects of temperature and guest molecule motions on this structure determination protocol for a variety of different systems are being investigated in greater detail, and it does not appear, in general, that motions necessarily compromise the method. For example, for a closely related system (low-loaded *p*-dibromobenzene in ZSM-5) we have carried out structure determinations with NMR data sets collected over a wider range of temperatures (180 to 300 K), and the same guest molecule locations were found at every temperature.⁴²

In the plots of the experimental CP rate constants against the calculated second moments, the linear correlation lines tend to have nonzero intercepts (see Figures 10, 12, and 15), which is not exactly consistent with the proportional relationship between k_{IS} and M_2 (eq 6). The reason for this anomaly, which was previously reported¹³ and seemed to disappear in some cases under certain conditions, is not entirely clear at present, and possible causes are currently being investigated. It is quite possible that the equations describing the CP and CP drain spin dynamics, and perhaps also the relationship between the CP rate constants and the second moments, which were developed primarily to describe $^1\text{H}/^{13}\text{C}$ spin systems in organic solids which have high densities of protons, are not completely valid for the $^1\text{H}/^{29}\text{Si}$ spin systems in these zeolite–sorbate complexes. Nevertheless, despite having nonzero intercepts in the correlation plots, it is clear that this NMR method correctly determines the locations of the guest molecules in these zeolite–sorbate complexes, and the general approach should be applicable to other systems.

Conclusions

We have shown that solid-state $^1\text{H}/^{29}\text{Si}$ CP MAS NMR can provide reliable structure determinations of zeolite–sorbate host–guest complexes and will be an important complement or alternative to XRD techniques, especially when crystals of suitable quality and size are not available. We have also demonstrated that structure determinations by solid-state NMR are still possible without measuring discrete internuclear distances. Since most real systems do not consist of isolated spin pairs, this solid-state NMR approach in which CP rate constants are correlated to second moments may be important in structural investigations of other types of materials, particularly host–guest systems, surface–molecule interactions, and interfacial phenomena in general. We have also demonstrated that the structure determination method is quite robust, with reliable structures determined from both relative and absolute CP rate constants obtained from $^1\text{H}/^{29}\text{Si}$ CP and CP drain data, respectively. The method is relatively independent of the exact atomic coordinates of the zeolite framework and appears to be relatively insensitive to well-defined motions of the guest molecules. Further detailed studies are underway to investigate the effects of motions on the structure determination method and to identify the source of the nonzero intercepts in the k_{IS} vs M_2 correlation plots. These experiments are also being extended to a variety of different guest molecules and zeolite hosts.

Acknowledgment. We thank the Natural Sciences and Engineering Research Council of Canada for Operating and Equipment Grants (C.A.F.) and for the award of a Postgraduate Fellowship (D.H.B.).

Supporting Information Available: Structure determination program used in the paper, implemented as a *Mathematica* notebook with a program outline, code and sample input files for the pDCB example (zip file); details of the determination of error ellipsoids to represent the scatter in atomic positions; atomic coordinates for the guest molecule location presented in Figure 9; $^1\text{H}/^{29}\text{Si}$ second moments calculated under different levels of guest molecule motion; tables and figures related to the structure determination carried out using the NMR data collected at 265 and 295 K. This material is available free of charge via the Internet at <http://pubs.acs.org>.